Università di Pisa

Modeling the effects of dephasing on mesoscopic noise

M. G. Pala
Dipartimento di Ingegneria dell'Informazione: Elettronica, Informatica, Telecomunicazioni, Università di Pisa
Giuseppe Iannaccone
Dipartimento di Ingegneria dell'Informazione: Elettronica, Informatica, Telecomunicazioni, Università di Pisa
Massimo Macucci
Dipartimento di Ingegneria dell'Informazione: Elettronica, Informatica, Telecomunicazioni, Università di Pisa
Giovanni Marola
Dipartimento di Ingegneria dell'Informazione: Elettronica, Informatica, Telecomunicazioni, Università di Pisa

M. G. Pala, G. Iannaccone, M. Macucci, G. Marola, Modeling the effects of dephasing on mesoscopic noise , (Invited) Noise and Information in Nanoelectronics, Sensors and Standard, II, vol. 5472, pp. 51-59, Gran Canaria, Spain 2004.

Modeling the effects of dephasing on mesoscopic noise

M.G. Pala[a], G. Iannaccone[a,b], M. Macucci[a,b] and G. Marola[a]

[a]Dipartimento di Ingegneria dell'Informazione, Università degli Studi di Pisa, and
[b]IEIIT-Consiglio Nazionale delle Ricerche,
via Caruso, I-56122 Pisa, Italy

ABSTRACT

We present simulations of the effects of dephasing on the shot noise properties of mesoscopic coherent devices, such as chaotic cavities and Aharonov-Bohm rings. We adopt a phenomenological model that exploits the statistical nature of the dephasing mechanism and is able to cover the intermediate regime between a fully coherent and completely incoherent (i.e., semiclassical) transport. By investigating conductance and noise properties as a function of the dephasing length, we conclude that decoherence has no specific effect on shot noise which can be distinguished from the one it has on conductance. In addition, when a large number of conducting channels is considered, semiclassical and quantum behavior must converge, yielding as a consequence the independence of DC and noise properties from dephasing.

Keywords: Shot noise, dephasing, mesoscopic transport, scattering matrix

1. INTRODUCTION

Phase coherence has a very important role in mesoscopic transport, in particular in the case of devices based on the wavelike behavior of electrons, such as electronic interferometric modulators,[1] and Aharonov-Bohm rings. The operation of such devices is possible because the evolution of the wave function, as predicted by the Schrödinger equation, is continuous and fully deterministic. However, decoherence due to the interaction between carriers and the environment[2] causes the loss of the predictability of the evolution of the system and may undermine the operation of such devices. Therefore, it is important to assess quantitatively the dependence of DC and noise properties of such devices on the dephasing length of the system l_ϕ, i.e., the length under which the electron loses quantum coherence, which yields information on the degree of decoherence of the system. The length l_ϕ can be typically determined, in the diffusive regime, by Weak Localization (WL)[3] measurements on various types of samples.[4]

Usually, ballistic transport in mesoscopic structures is addressed in the framework of the Landauer-Büttiker theory of transport,[5] which does not allow to include directly the effects of dephasing. Such effects are usually treated with phenomenological models, which are based on the insertion of a virtual voltage probe[6] into the ballistic region: electrons traveling from source to drain can be absorbed by the third probe, where they lose their phase information before being re-injected into the conductor. Such proposal was generalized in order to address a non local treatment of decoherence, both considering a probe with infinite modes and vanishing tunneling rate[7] and considering an arbitrary number of probes uniformly distributed in the device domain.[8] Alternatively, the effect of dephasing can be modeled by adding an imaginary potential to the Hamiltonian in the device region,[9,10] which acts as an absorber of the wave function, and introducing an adequate mechanism for the re-injection of phase-randomized particles, in order to ensure continuity of the total current probability density.

An alternative phenomenological method that treats decoherence as a phase randomizing statistical process has been recently proposed and implemented with a Monte Carlo technique.[11] Such technique is based on a phenomenological microscopic model, which captures the effect of elastic interactions in terms of a random

Send correspondence to
Marco Pala, Dipartimento di Ingegneria dell'Informazione, Università degli Studi di Pisa, via Caruso, 56122 Pisa, Italy.
Tel.: +39 050 2217639. Fax: +39 050 2217522.
E-mail: m.pala@iet.unipi.it

Noise and Information in Nanoelectronics, Sensors, and Standards II, edited by Janusz M. Smulko, Yaroslav Blanter, Mark I. Dykman, Laszlo B. Kish, Proc. of SPIE Vol. 5472 (SPIE, Bellingham, WA, 2004) · 0277-786X/04/$15 · doi: 10.1117/12.548604

term added to the phase of the single particle wave function. Given the random character of scattering events, each Monte Carlo run provides a particular occurrence of the reduced single particle scattering matrix. Average transport properties are obtained from large samples of Monte Carlo runs.

From the modeling point of view, researchers typically have to simplify the transport model, reducing it to the limit of complete coherence, or to the opposite limit of incoherent transport using a semiclassical model that does not address interference effects. In general terms, if the Fermi wave length approaches zero or the number of conducting channels N tends to infinity, and the conductance is much larger that the conductance quantum e^2/h, approaches based on completely coherent transport yield the same result as semiclassical approaches, due to the correspondence principle.

As far as shot noise is concerned, even for finite N, approaches based on completely coherent transport often yield the same result as semiclassical ones. Such is the case, for example, of the so-called 1/3 suppression of shot noise in diffusive conductors, which was obtained both with a quantum mechanical theory, such as Random-Matrix Theory (RMT),[13] and in semiclassical terms, using the Boltzmann-Langevin equation.[14] Similar agreement has been obtained for the so-called 1/4 suppression of shot noise in chaotic cavities,[15,16] and also for shot noise in single-electron transistors and resonant tunneling structures.[17–19]

In this paper, we investigate the effect of dephasing on shot noise properties of chaotic cavities and Aharonov-Bohm rings by means of numerical simulations based on the above mentioned statistical model for dephasing. In such a way, we are able to explore the whole regime between completely coherent and completely incoherent transport. We observe a constant level of shot noise as a function of the dephasing length only for the case of few propagating modes. We find, for a very small number of propagating modes in the channel, a dependence of shot noise and conductance on l_ϕ. However, as we increase the number of open channels, conductance and noise properties become simultaneously independent of the dephasing length. This allows us to conclude that, at least in the cases we have examined, shot noise does not contain additional information on decoherence with respect to that already contained in the conductance. In Sec. 2 we present the statistical approach to dephasing in the scattering matrix formalism, and in Sec. 3 we show numerical results for a mesoscopic cavity that in the classical limit presents chaotic behavior and for an Aharonov-Bohm ring that is used for its interference properties in mesoscopic physics. Finally, in Sec. 4 we provide our conclusions and final considerations.

2. MODEL

In this Section we present a phenomenological approach for including dephasing in the simulation of mesoscopic devices based on the scattering matrix technique. Such method treats decoherence as a random fluctuation of the phase of the propagating modes involved in the computation of the scattering matrix, and enables us the obtain average conductances and noise spectra from a sufficiently large ensemble of Monte Carlo simulations. Here, we just provide a brief overview of the model; details can be found in a previous paper.[11]

The model has been developed within the framework of the Landauer-Büttiker theory[5] of transport in mesoscopic devices. The conductance of a generic device is related to the transmission probability matrix $T = tt^\dagger$ by the formula

$$G = g\frac{e^2}{h}\sum_n T_n \,, \tag{1}$$

where t is the transmission amplitude matrix, g is a degeneracy factor ($g = 2$ in our case due to spin degeneracy) and the sum is over the all the eigenvalues T_n of the transmission probability operator T.

The device domain is discretized and then divided into a number of slices N_x along the propagation direction (i.e. the x-axis). The electronic wave function at the j-th slice reads

$$\psi_j(x,y) = \sum_n \frac{\chi_{j,n}(y)}{\sqrt{\hbar k_{j,n}/m_j}}\left(a_{j,n}e^{ik_{j,n}x} + b_{j,n}e^{-ik_{j,n}x}\right) \,, \tag{2}$$

where $\chi_{j,n}(y)$ are the transverse eigenvectors with eigenenergies $E_{j,n}$ and the longitudinal wave vectors $k_{j,n}$ are related to the total energy E by the condition $E = E_{j,n} + \hbar^2 k_{j,n}^2/2m_j$. The wave function normalization of Eq. (2) corresponds to unitary current probability. The sets of coefficients $a_{j,n}$ and $b_{j,n}$ represent the transmission and

reflection amplitudes in the j-th slice, and can be obtained by enforcing the continuity of the wave function and of the current density at the interface between the j-th and the $(j+1)$-th slice. The scattering matrix S_j relates the coefficients of the wave functions of the j-th and $(j+1)$-th slices as follows:

$$\begin{pmatrix} b_j \\ a_{j+1} \end{pmatrix} = S_j \begin{pmatrix} a_j \\ b_{j+1} \end{pmatrix} = \begin{pmatrix} r & t' \\ t & r' \end{pmatrix} \begin{pmatrix} a_j \\ b_{j+1} \end{pmatrix}, \tag{3}$$

where the symbols t, t', r and r' indicate the transmission and reflections matrices. The composition between two adjacent scattering matrices S_1 and S_2 yields a matrix $S = S_1 \otimes S_2$ with transmission and reflection matrices given by:

$$\begin{aligned} r &= r_1 + t_1'(1 - r_2 r_1')^{-1} r_2 t_1 \\ t &= t_2(1 - r_1' r_2)^{-1} t_1 \\ t' &= t_1'(1 - r_2 r_1')^{-1} t_2' \\ r' &= r_2' + t_2(1 - r_1' r_2)^{-1} r_1' t_2' \,. \end{aligned} \tag{4}$$

The total scattering matrix of the structure S is given by the composition $S = S_1 \otimes S_2 \otimes \cdots \otimes S_{N_x - 1}$, where the symbol $\otimes$ represents the operation described by Eqs. (4).

The presence of a magnetic field $\mathbf{B} = B\hat{\mathbf{z}}$ perpendicular to the propagation plane xy, can be taken into account by adopting the transverse gauge $\mathbf{A} = Bx\hat{\mathbf{y}} = A(x)\hat{\mathbf{y}}$ for the vector potential $\mathbf{A} = \nabla \times \mathbf{B}$. The new Hamiltonian can be written as the sum of two terms: $H(x,y) = H_{\text{trans}}(y) + H_{\text{long}}(x)$, where $H_{\text{trans}} = [p_y - eA(x_j)]^2/2m_y + V(y)$ refers to the transversal part of the Hamiltonian and $H_{\text{long}} = p_x^2/2m_x$ to the longitudinal one. The eigenvectors are given by the product of the eigenvectors for the two Hamiltonians, that are plane waves for H_{long} and the vectors

$$\chi_{n,j}(y) = \chi^0_{n,j}(y)\, \exp[-ieA(x_j)y/\hbar] \tag{5}$$

for H_{trans}, where $\chi^0_{n,j}(x)$ are the solutions in the case $B = 0$. Furthermore, with this gauge, the eigenvalues $E_{j,n}$ are not altered by the presence of the magnetic field. We note that the condition for the validity of the discretization of H_{trans} is that the magnetic flux through a generic slice $[A(x_{j+1}) - A(x_j)]W$ is much smaller than the quantum unit of flux h/e, where W is the transverse device length.[20]

We introduce in our description the effects of decoherence as a dephasing of the wave function in Eq. (2). The coherent propagation through the j-th slice is described by a diagonal transmission matrix with elements $e^{ik_{j,m}d_j}\delta_{mn}$, where $d_j = x_{j+1} - x_j$. We modify the transmission matrix by adding to each diagonal term a random phase ϕ_{R} so that the generic element of the transmission matrix becomes

$$t_{mn} = e^{i(k_{j,m}d_j + \phi_{\text{R}})}\delta_{mn}. \tag{6}$$

ϕ_{R} is extracted by a random number generator and obeys a zero average Gaussian distribution with variance $\sigma_j^2 = d_j/l_\phi$.

The scattering matrix obtained in such a way only represents a particular occurrence of the reduced scattering matrix of the single particle. The average reduced scattering matrix is obtained by averaging the conductance over a sufficient number of runs, typically of the order of one hundred. In this way we take into account the intrinsic statistical character of the dephasing process. We emphasize that the usual properties of the scattering matrix S, such as unitarity

$$SS^\dagger = I \tag{7}$$

and the Onsager-Casimir relations,[21] valid for a multi-probe conductor,

$$T_{pq}(\mathbf{B}) = T_{qp}(-\mathbf{B}) \tag{8}$$

$$R_{pp}(\mathbf{B}) = R_{pp}(-\mathbf{B}) \tag{9}$$

still hold.[11] In Eq. (8,9) T_{pq} and R_{qq} are the transmission and reflection probabilities between the leads denoted by labels p and q.

3. NUMERICAL RESULTS

In this Section we apply the phenomenological model described in Sec. 2 to a chaotic cavity and to an Aharonov-Bohm ring and compute the conductance and noise properties as a function of the dephasing length l_ϕ.

We consider a system out of equilibrium and are interested in the shot noise of a two-terminal sample at zero temperature. Using the scattering matrix representation and its unitarity,[22] we obtain the general expression of the low noise spectral density of shot noise

$$S_N = \frac{2e^2}{h}\mathrm{Tr}[r^\dagger r t^\dagger t]e|V| = \frac{2e^2}{h}\mathrm{Tr}[(I - t^\dagger t)t^\dagger t]e|V| \,, \tag{10}$$

where V is the voltage applied between the leads and the symbol $\mathrm{Tr}[T]$ indicates the trace of the matrix T. Equation (10), in the basis of the eigenvalues T_n (with $n = 1, ..., N$) of the transmission operator $T = t^\dagger t$ reads

$$S_N = \frac{2e^3|V|}{h}\sum_n T_n(1 - T_n) \,. \tag{11}$$

In the case of small transmission of all modes ($T_n \ll 1, \forall n$) we recover the so-called "full" shot noise spectrum

$$S_{\mathrm{full}} = \frac{2e^3|V|}{h}\sum_n T_n \,. \tag{12}$$

In particular, neither closed ($T_n = 0$) nor open ($T_n = 1$) channels contribute to the sum in Eq. (11), whereas the maximum contribution arises from channels with $T_n = 1/2$. The shot noise spectral density S_N is always smaller than or equal to S_{full} and therefore it is convenient to define the noise suppression factor or Fano factor as

$$\gamma \equiv \frac{\sum_n T_n(1 - T_n)}{\sum_n T_n} \,, \tag{13}$$

which can be interpreted as a signature of quantum correlations, in our case due to the fermionic nature of charge carriers.

First, we consider a circular GaAs quantum dot with a diameter of 1.5 μm connected to two leads with a width of 50 nm, which is known to exhibit a Fano factor of 1/4, as obtained by both quantum and semiclassical models for $N \gg 1$.[12] The transmission probability T_n of each channel obeys the distribution function $P(T_n)$, which can be computed using RMT[15,16] and is given by

$$P(T_n) = \frac{1}{\pi}\frac{1}{\sqrt{T_n(1 - T_n)}} \,. \tag{14}$$

Equation (14) indicates that almost open ($T_n \approx 0$) and almost closed ($T_n \approx 1$) channels are preferred with respect to the others. Given the large number of propagating channels involved in calculations, it is convenient to express the conductance and the Fano factor in terms of the first two moments of the transmission probability. Using Eq. (14), we obtain $\langle T_n \rangle = 1/2$ and $\langle T_n(1 - T_n) \rangle = 1/8$, which yield the conductance value

$$G = \frac{2e^2}{h}\frac{N}{2} \,, \tag{15}$$

where N is the number of conducting modes in the leads. Similarly, we obtain the Fano factor $\gamma = 1/4$, which, when the number of conducting channels in the left lead N_L is different from the one on the right lead N_R, can be generalized to the expression

$$\gamma = \frac{N_L N_R}{(N_L + N_R)^2} \,. \tag{16}$$

In the case of completely incoherent transport regime a result identical to Eq. (16) is obtained by solving the semiclassical Boltzmann-Langevin equation.[23]

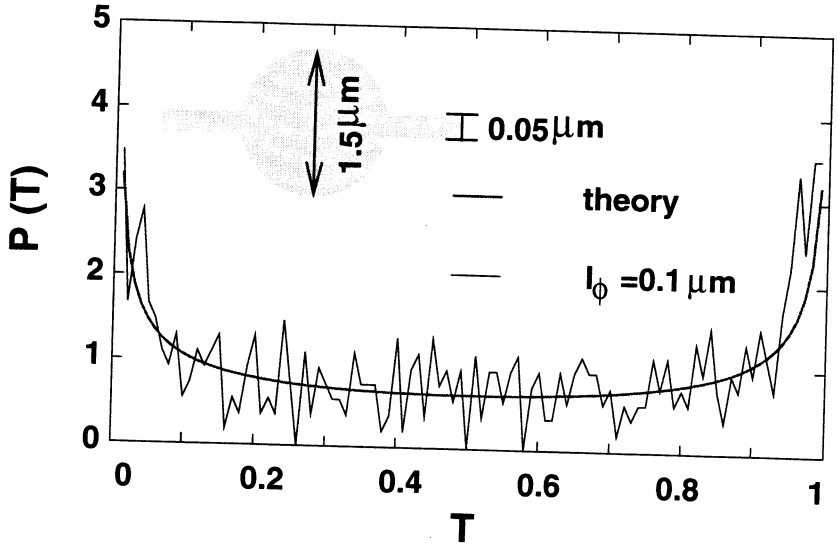

Figure 1. Distribution of the transmission matrix eigenvalues for a symmetric cavity with 9 propagating channels in the leads, for $l_\phi = 0.1$ μm. The cavity has a radius of 750 nm and leads have a width of 50 nm (shown in the inset). Thick line: distribution obtained from an ensemble of 100 Monte Carlo runs; thin line: distribution provided by RMT.

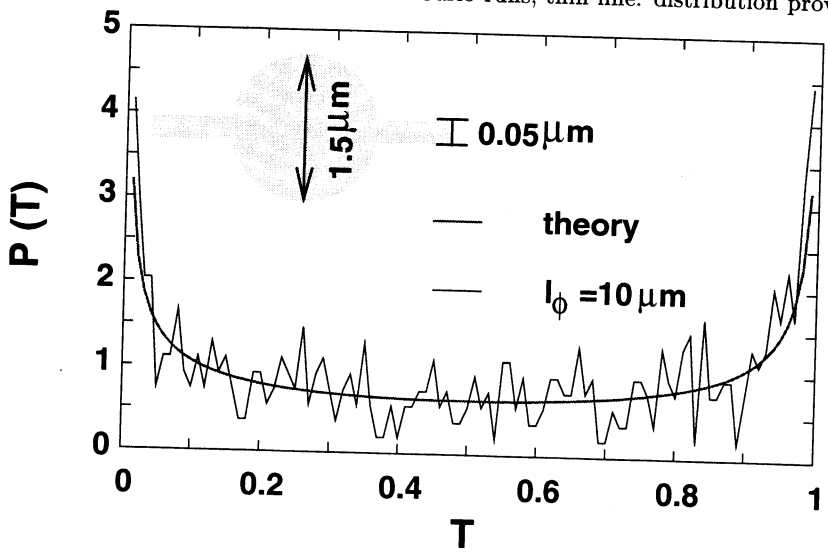

Figure 2. Distribution of the transmission matrix eigenvalues for a symmetric cavity with 9 propagating channels in the leads, for $l_\phi = 10$ μm. The cavity has a radius of 750 nm and leads have a width of 50 nm (shown in the inset). Thick line: distribution obtained from an ensemble of 100 Monte Carlo runs; thin line: distribution provided by RMT.

We recover the same distribution when the transmission probability is computed for $l_\phi \gg L$ and for $l_\phi \ll L$, where L is the device size. In Fig. 1 we show the probability distribution $P(T_n)$ of the symmetric cavity with 9 conducting channels in the leads, and more than 250 in the center of the cavity for the case of a dephasing length $l_\phi = 0.1$ μm, a completely incoherent regime. Similarly, in Fig. 2 we show the same quantity for the case of $l_\phi = 10$ μm, that is transport regime with a larger degree of coherence. The details of the two distributions are very similar and are in very good agreement with the analytical expression of Eq. (14), given by the thick line.

In Fig. 3 we show how the conductance G of the quantum dot is modified by the effect of decoherence. We

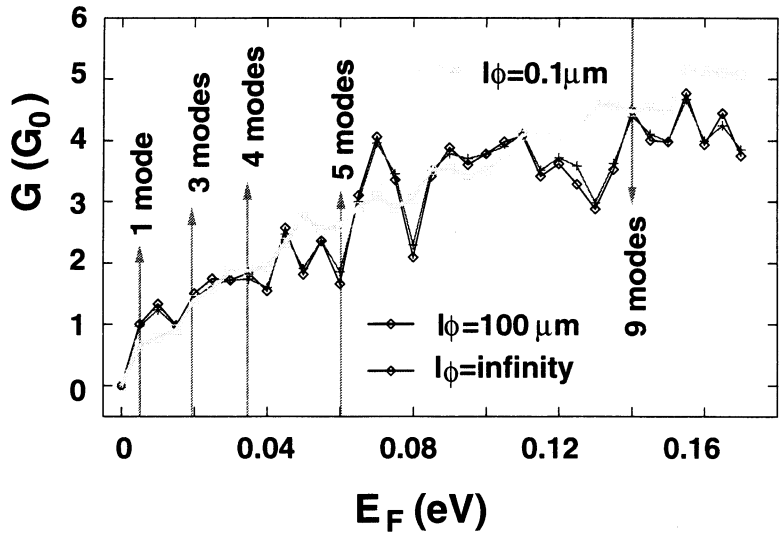

Figure 3. Conductance of the chaotic cavity shown in the inset of Fig. 1,2 versus the Fermi energy E_F. The lines correspond to the case of $l_\phi = \infty$, $l_\phi = 100$ μm (thin line) and $l_\phi = 0.1$ μm (thick line). The various points labeled with arrows indicate the values of the Fermi energy for which the Fano factor of Fig. 4 is computed.

plot both the case of coherent transport ($(l_\phi = \infty)$, and of quasi-coherent transport ($l_\phi = 100$ μm), characterized by large fluctuations of G as a function of the Fermi energy (the so-called universal conductance fluctuations), and the case of incoherent transport with $l_\phi = 0.1$ μm that is characterized by a staircase behavior. In particular, we note that the conductance steps for large N become close to $G_0/2 = e^2/h$, as predicted by Eq. (15).

In Fig. 4 we show the most important result of the paper: the dependence of the Fano factor of the chaotic cavity on the dephasing length l_ϕ, which indicates the degree of coherence of the system. From the bottom to the top we show the results obtained at the fixed Fermi energies labeled by arrows in the conductance staircase of Fig. 3. As a first comment, we observe that for $N \geq 3$ the Fano factor and the conductance are practically independent of the dephasing length and therefore shot noise measurements cannot provide additional information on phase coherence with respect to DC measurements. This is connected to the fact that the different degree of coherence does not alter the transmission distribution $P(T_n)$, as shown in Figs. 1,2. Conversely, we observe that the Fano factor, when the conductance is of the order of the fluctuation magnitude, strongly depend on the dephasing length.

In order to confirm our previous results, we consider a second mesoscopic structure, an Aharonov-Bohm ring with an external radius of 750 nm, an internal radius of 450 nm and a lead width of 50 nm. Such a structure can be obtained from the previous quantum dot by adding a central antidot, it is used in experiments on quantum interference and exhibits a sensitive resonance phenomenon.

In Fig. 5 we sketch the Fano factor for the same energy values used for the chaotic cavity. Also in this case we find that the dephasing mechanism, when the number of open channels is large enough, does not affect the Fano factor, which is slightly larger than 0.25. Again, in the case of a single propagating mode in the structure we note a dependence of the average value of the Fano factor, confirming a dependence on dephasing when conductance is dominated by a resonance, and is also affected by dephasing.

4. CONCLUSIONS

In this paper, we considered ballistic structures such as chaotic cavities and Aharonov-Bohm rings, and computed the dependence of conductance and noise on the degree of phase coherence in the system. We have developed a novel method that exploits the statistical nature of the decoherence mechanisms by adding a random term to the phase accumulated by the carriers traveling in the conductor and then performing a statistical average over

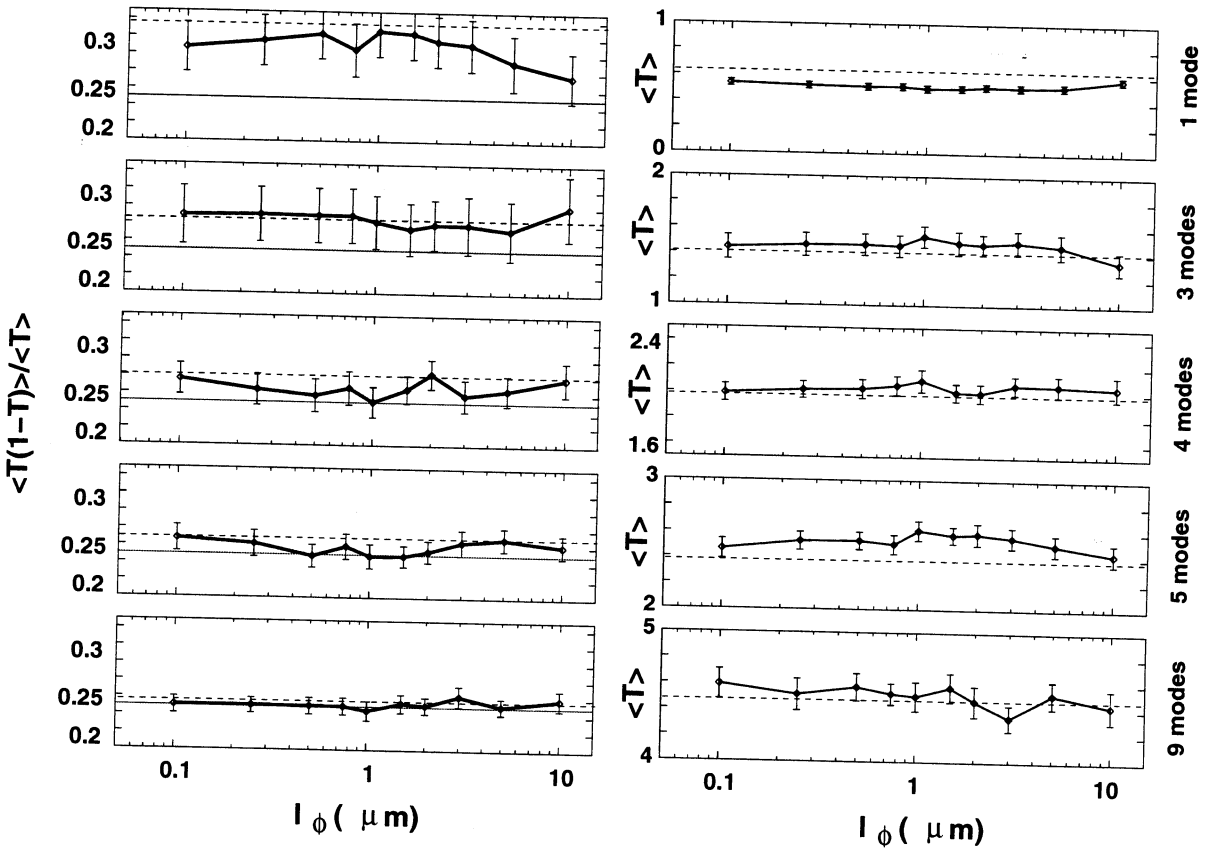

Figure 4. Left: the Fano factor $\langle T(1-T)\rangle/\langle T\rangle$ of the chaotic cavity as a function of the dephasing length for different energies corresponding to various number of propagating channels in the leads. Dashed lines indicate the level of Fano factor and conductance for a small energy range around E_F. From the bottom to the top the cases for $N = 9, 5, 4, 3, 1$ are shown. The error bars in the plot are computed assuming a tolerance range around the mean value of $\pm 2s_e$, where s_e is the standard error of the sample of data, computed as the ratio of the sample's standard deviation σ_s to the square root of the number of runs. Right: the conductance of the same structure versus l_ϕ.

many occurrences of such random variations. We show that the model is able to address an arbitrary degree of phase coherence in the transport model, and to recover known results in the limits of fully quantum mechanical and semiclassical calculations. The effect of phase coherence on shot noise appears to be limited to the case of few propagating modes, when also conductance is affected. Therefore, we conclude that noise properties do not provide additional information on the degree of coherence beyond that obtainable from DC properties.

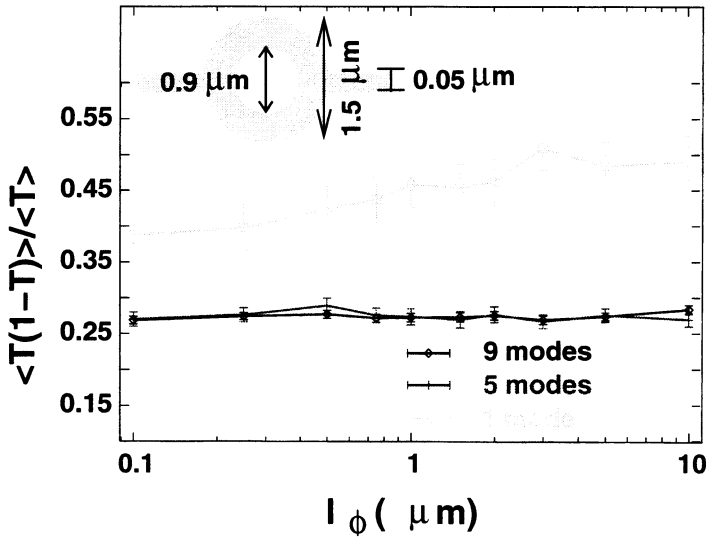

Figure 5. Fano factor $\langle T(1-T)\rangle/\langle T\rangle$ of the Aharonov-Bohm ring a function of the dephasing length for different energies. From the bottom to the top we show only the cases corresponding to $N = 9, 5, 1$. The device is obtained from the quantum dot sketched in Fig. 1,2 by the insertion of a central antidot of a diameter of 0.9 μm (shown in the Inset).

ACKNOWLEDGMENTS

Financial support from the IST NanoTCAD project (EC contract IST-1999-10828) is gratefully acknowledged.

REFERENCES

1. F. Sols, M. Macucci, U. Ravaioli, and K. Hess, "On the possibility of transistor action based on quantum interference phenomena", *Appl. Phys. Lett.*, **54**, 350-2, 1989.
2. A. Stern, Y. Aharonov, and Y. Imry, "Phase uncertainty and loss of interference: A general picture" *Phys. Rev. A*, **41**, 3436-3448, 1990.
3. B.L. Altshuler, A.G. Aronov, and D. Khmelnitskii, "Effects of electron-electron collisions with small energy transfers on quantum localisation", *J. Phys. C*, **15**, 7367-7386, 1982.
4. C.W.J. Beenakker and H. van Houten in *Solid State Physics, vol. 44, Semiconductor Heterostructures and Nanostructures* (Academic Press, San Diego, 1991) pags. 1-228.
5. R. Landauer, IBM J. Res. Dev. , 1, 233 (1957); M. Büttiker, "Four-Terminal Phase-Coherent Conductance", *Phys. Rev. Lett.*, **57**, 1761-4, 1986.
6. M. Büttiker, "Role of quantum coherence in series resistors", *Phys. Rev. B*, **33**, 3020-6, 1986.
7. P. W. Brouwer and C.W.J. Beenakker, "Voltage-probe and imaginary-potential models for dephasing in a chaotic quantum dot", *Phys. Rev. B*, **55**, 4695-4702, 1997.
8. T. Ando, "Crossover between quantum and classical transport: quantum Hall effect and carbon nanotubes", *Physica E*, **20**, 24-32, 2003.
9. G. Czycholl and B. Kramer, "Nonvanishing zero temperature static conductivity in one dimensional disordered systems", *Solid State Comm.*, **32**, 945-951, 1979.
10. K. B. Efetov, "Temperature Effects in Quantum Dots in the Regime of Chaotic Dynamics", *Phys. Rev. Lett.*, **74**, 2299-2302, 1995.
11. M.G. Pala and G. Iannaccone, "Statistical model of dephasing in mesoscopic devices introduced in the scattering matrix formalism", to be published on *Phys. Rev. B.* Preprint: cond-mat/0312478
12. Y. Blanter and M. Büttiker, "Shot noise in mesoscopic conductors", *Phys. Rep.*, **336**, 1-166, 2000.
13. C.W.J. Beenakker and M. Büttiker, "Suppression of shot noise in metallic diffusive conductors", *Phys. Rev. B*, **46**, 1889-1892, 1992.

14. N.E. Nagaev, "On the shot noise in dirty metal contacts", *Phys. Lett. A*, **169**, 103-7, 1992.
15. H.U. Baranger and P. Mello, "Mesoscopic transport through chaotic cavities: A random S-matrix theory approach", *Phys. Rev. Lett.*, **73**, 142-5, 1994.
16. R.A. Jalabert, J.-L. Pichard, and C.W.J. Beenakker, "Universal quantum signatures of chaos in ballistic transport", *Europhys. Lett.*, **27**, 255-60, 1994.
17. M. Büttiker, "The quantum phase of flux correlations in waveguides", *Physica B*, **175**, 199-212, 1991.
18. L.Y. Chen and C.S. Thing, "Theoretical investigation of noise characteristics of double-barrier resonant-tunneling systems", *Phys. Rev. B*, **43**, 4534-7, 1991.
19. G. Iannaccone, M. Macucci, B. Pellegrini, "Shot noise in resonant tunneling structures, *Phys. Rev. B*, **55**, 4539-4551, 1997.
20. M. Governale and D. Boese, "Magnetic barrier in confined two-dimensional electron gases: Nanomagnetometers and magnetic switches", *Appl. Phys. Lett.*, **77**, 3215-7, 2000.
21. L. Onsager, "Reciprocal Relations in Irreversible Processes", *Phys. Rev.*, **38**, 2265-2279, 1931; H.B.G. Casimir, "On Onsager's Principle of Microscopic Reversibility", *Rev. Mod. Phys.*, **17**, 343-350, 1945.
22. M. Büttiker, "Scattering theory of thermal and excess noise in open conductors", *Phys. Rev. Lett.*, **65**, 2901-4, 1990.
23. Ya.M. Blanter and E.V. Sukhorukov, "Semiclassical Theory of Conductance and Noise in Open Chaotic Cavities", *Phys. Rev. Lett.*, **84**, 1280-3, (2000).